Turkish Journal of Chemistry

http://journals.tubitak.gov.tr/chem/

Research Article

Turk J Chem
(2019) 43: 197 – 212
© TÜBİTAK
doi:10.3906/kim-1807-139

New diazo-containing phenolic oximes: structural characterization, computational studies, and solvent extraction of Cu(II), Ni(II), and Zn(II) ions

Muharrem KARABÖRK[1], **Hilal KIRPIK**[1], **Koray SAYIN**[2], **Muhammet KÖSE**[1,*]
[1]Department of Chemistry, Kahramanmaraş Sütçü İmam University, Kahramanmaraş, Turkey
[2]Department of Chemistry, Institute of Science, Cumhuriyet University, Sivas, Turkey

Received: 31.07.2018 • **Accepted/Published Online:** 09.11.2018 • **Final Version:** 05.02.2019

Abstract: In the current study, four new phenolic oxime ligands (HL1ox–HL4ox) containing diazo groups (-N=N-) were synthesized and used for liquid-liquid extraction of heavy metal ions [Cu(II), Ni(II), and Zn(II)]. The new compounds were characterized by analytical and spectroscopic methods. Solid-state structures of HL1ox–HL3ox were determined by single-crystal X-ray diffraction studies. Hirshfeld surface analysis of the compounds was performed to determine the contribution of different intermolecular contacts to the stability of the structures. The HL1ox–HL4ox ligands showed higher extraction performance for Cu(II) ion than Ni(II) and Zn(II) ions. The effect of pH on extraction capacity was investigated and the oxime compounds showed high extraction capacity at low pH values. The effects of the substitute groups (at the meta position of the phenol ring) on the extraction were investigated. Within the oxime ligands, the HL3ox compound exhibited higher extraction capacity for Cu(II) ions. The better extraction value of HL3ox is attributed to the weak hydrogen bond type interactions, which result in more stable complexes.

Key words: Solvent extraction, Cu(II) ion, phenolic oxime, computational studies

1. Introduction

Hydrometallurgy is often preferred to conventional pyrometallurgy by industry since it usually results in excellent materials and energy balances because of the reusability of the reagents.[1] A hydrometallurgical process usually involves three main operations: leaching, concentration and separation, and reduction. First of all, the metal ore is solved in an aqueous medium (leaching), and then the metal to be recovered is separated and concentrated using liquid-liquid extraction and the resulting high-purity aqueous solution is reduced to generate the metal.[2] Solvent extraction has been widely applied to extract valuable metals from ore processing.[3] The solvent extraction in extractive hydrometallurgy has commercial importance.[4] Conventionally, to recover the base metal, metal cations are transferred selectively to a water-immiscible phase by using ion-exchanger ligands, which release an equivalent number of cations, usually protons, back to the aqueous feed solution.[5] Among the most commercially successful cation exchange reagents are phenolic oxime reagents, which are used for copper recovery from sulfate streams.[6] Copper production using phenolic oxime extractants accounts for approximately 25% of copper production in the world.[7] The sensitivity and selectivity of phenolic oxime extractants for Cu(II) compared to other base metal ions results from the more stable pseudomacrocyclic structure of the copper complex (Figure 1).

*Correspondence: muhammetkose@ksu.edu.tr

This work is licensed under a Creative Commons Attribution 4.0 International License.

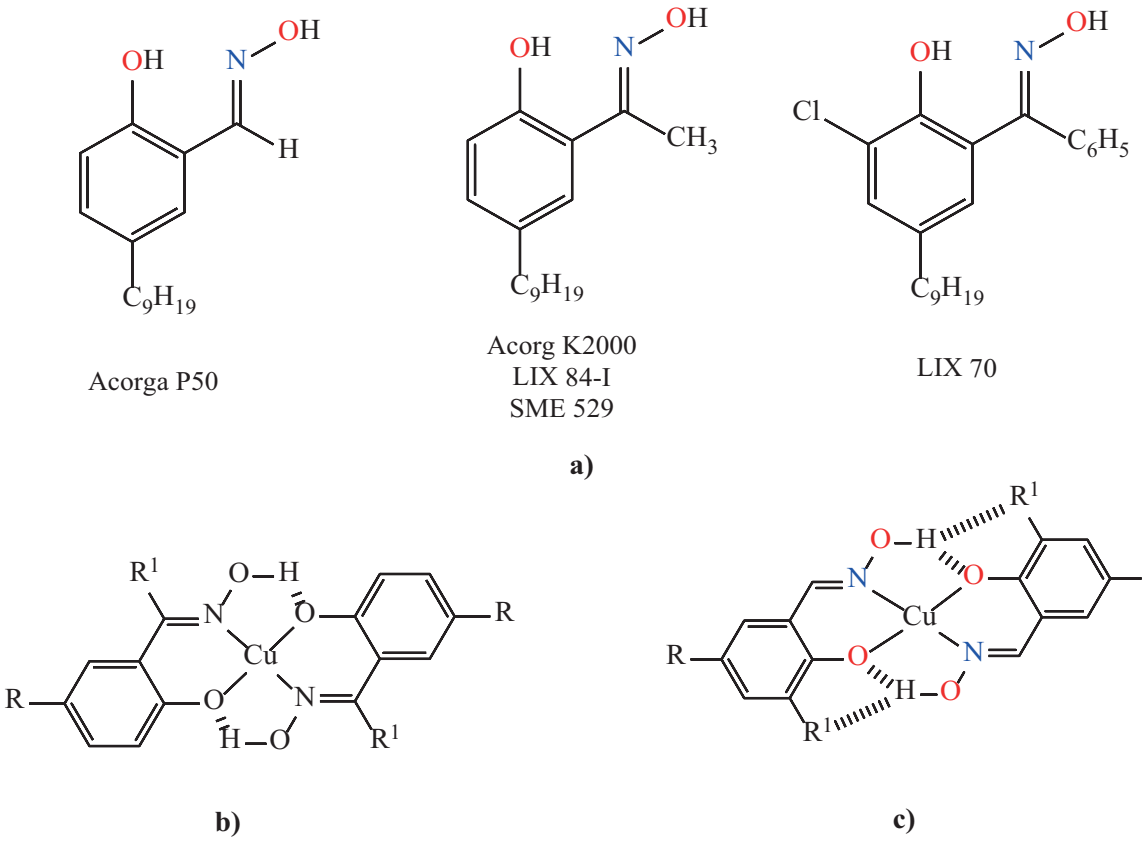

Figure 1. a) Examples of commercially available phenolic oxime extractants, b) general sutructure of Cu(II) complexes, and c) interligand buttress of hydrogen bonding.

Formation of the strong interligand hydrogen bonds between the oxime hydrogen and the phenolic oxygen atoms provides a planar donor set and a suitable cavity for Cu(II).[8–10] There are also mixtures used for the extraction of heavy metals. Moore et al., for example, employed HDNNS (dinonylnaphthalene sulfonic acid) and Lix63 (5,8-diethyl-7-hydroxy-6-dodecanone oxime) for the extraction of copper(II) from iron(III).[8–10] Recently, Zhu et al. used a mixture of dinonylnaphthalene sulfonic acid and n-hexyl 3-pyridinecarboxylate ester for the extraction of Cu(II) from aqueous solution. The mixture showed synergistic solvent extraction for Cu(II).[8–10] Intermolecular interactions between extractants, such as hydrogen bonds, have a significant effect on the stability of complexes that form in the water-immiscible phase, and buttressing of interligand hydrogen bonding control cavity sizes consequently can be very effectively used to tune strengths of saliclylaldoxime extractants.[11] The usage of highly selective and stable extractants for a specific metal is critical for reducing production cost, enhancing product quality, and minimizing the environmental impact.[12]

In this work, four new azo-aldehyde compounds (HL1–HL4) and their oxime derivatives (HL1ox–HL4ox) were synthesized and characterized. The HL1ox–HL4ox compounds were used for solvent extraction of metal ions. The effects of time and pH on the extraction capacity were investigated in detail.

2. Results and discussion

In this work, four new azo-aldehyde compounds, HL1–HL4, and their oxime derivatives, HL1ox–HL4ox, were synthesized and characterized by spectral and analytical methods. In the azo-aldehyde synthesis, the diazonium

salts of the *p*-substituted aniline compounds were prepared using hydrochloric acid and sodium nitrite followed by the coupling reaction with salicylaldehyde derivatives. The oxime compounds (HL1ox–HL4ox) were obtained by the condensation reaction of the azo-aldehyde compounds with hydroxylamine in ethanol.[13] The synthesis reaction of the azo-aldehyde and their oxime derivatives is shown in Figure 2.

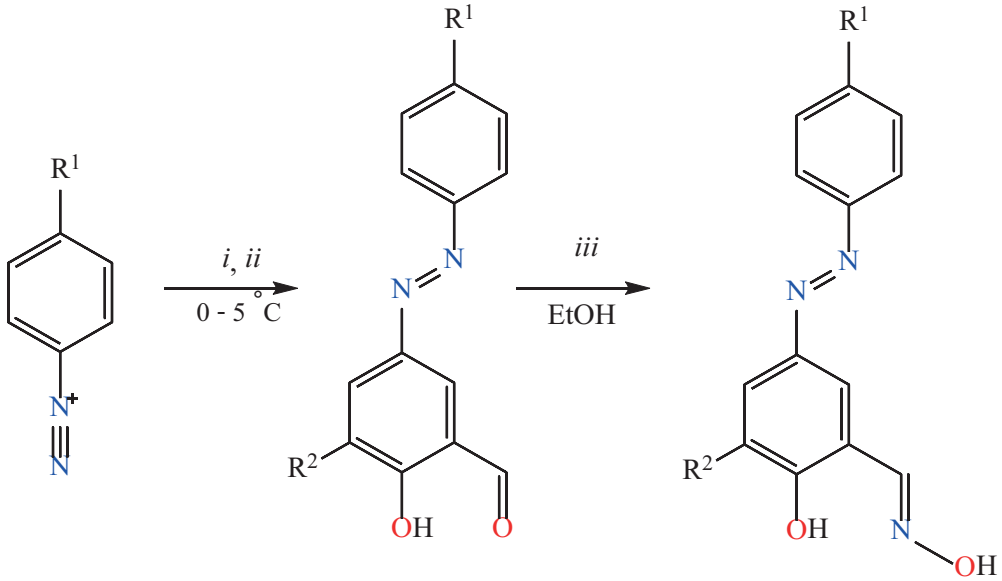

Figure 2. The synthesis of new HL1ox–HL4ox (*i* = NaOH (10%), *ii* = 2-hydroxybenzaldehyde, 3-tert-butyl-2-hydroxybenzaldehyde, 2-hydroxy-3-methoxybenzaldehyde, 2-hydroxy-3-methylbenzaldehyde, *iii* = NaOAc and $NH_2OH.HCl$).

The synthesized aldehyde and oxime compounds were characterized by ^1H and ^{13}C NMR, FTIR spectroscopy, and elemental analysis (CHN). The CHN data are in good agreement with calculated values. Single crystals of HL1ox–HL3ox compounds were grown from slow evaporation of MeOH solutions of the compounds. The solid-state structures of these compounds were determined by single-crystal X-ray diffraction (XRD) studies.

2.1. NMR spectra

The characterization of the synthesized azo-aldehyde compounds (HL1–HL4) was carried out by ^1H and ^{13}C NMR spectra and obtained data are given in the experimental section. In the spectra of the compounds, signals due to the phenolic-OH protons were observed in 11.33–12.15 ppm range. The singlet signals in the 10.01–10.05 ppm range are due to the protons of the aldehyde group (H-CO-). The aromatic protons of the compounds were observed in the range between 7.13 and 8.23 ppm. In the ^1H spectra of HL1 and HL2, the multiplet signals due to the ethyl group ($-CH_2CH_3$) protons were observed in the 1.32–1.33 and 2.76–2.77 ppm ranges. For HL2, tert-butyl group ($-C(CH_3)_3$) protons were observed as a singlet peak at 1.53 ppm. The methoxy group ($-OCH_3$) protons of HL3 were observed at 1.53 ppm. The singlet peaks observed at 1.41 and 2.38 ppm in the spectrum of HL4 are due to the protons of the tert-butyl ($-C(CH_3)_3$) and ($-CH_3$) group protons, respectively.

The ^1H NMR spectra of the four synthesized *p*-substituted phenolic oxime compounds (HL1ox–HL4ox) were measured in $CDCl_3$. The integration values are in good agreement with the number of protons present in the compounds and there are no organic impurities in the samples. The carbonyl group (-CH=O) proton

signals observed in the spectrum of the azo-aldehyde compounds (HL1–HL4) in the range of 10.01–1.05 ppm completely disappeared in the ^{1}H NMR spectra of the oxime compounds. Instead, new singlet signals due to the azomethine (-CH=N) group proton were seen in the 8.36–8.38 ppm range. The singlet signals observed at 10.28, 10.79, 10.35, and 10.52 ppm in the HL1ox–HL4ox spectra of the compounds, respectively, are due to the phenolic proton (Ph-OH).

In the ^{13}C NMR spectra of HL1–HL4, the characteristic carbonyl group (-CH=O) carbon signals were observed at 196.60, 197.28, 196.35, and 196.73 ppm, respectively. The ethyl group (-CH_2CH_3) carbon signals in the spectra of HL1 and HL2 compounds were seen in the 15–29 ppm range. The peaks observed at 29.18 ppm and 35.20 ppm in the spectrum of HL2 confirmed the presence of the tert-butyl (-$C(CH_3)_3$) group in the compound. The methoxy group carbon signal in the spectrum of HL3 was observed at 56.40 ppm. The carbon atom of the methyl (-CH_3) group in the HL4 compound was observed at 15.25 ppm and the presence of the tert-butyl group (-$C(CH_3)_3$) in the compound was confirmed by the peaks observed at 31.29 and 35.04 ppm. The carbon atom signals in the aromatic rings of the compounds (HL1–HL4) were observed in the range of 117.92–154.69 ppm. In the ^{13}C NMR spectra of the oxime compounds (HL1ox–HL4ox), the carbonyl group (-CH=O) carbon atom signal was completely absent and, instead, oxime group (-C = N-OH) carbon signals in the range of 158 to 159 ppm were observed. The rest of the carbon atom signals are in good agreement with their proposed structures.

2.2. FTIR spectra

FTIR spectra of the compounds were obtained to determine the characteristic vibration bands and the obtained data are given in the experimental section. The carbonyl group í(C=O) vibrations in the spectra of HL1–HL4 were observed as sharp peaks at 1652, 1646, 1666, and 1651 cm^{-1}, respectively. The vibration band of the N=N bond was observed in the 1426–1460 cm^{-1} range. The O-H stretching vibrations of the phenolic groups in the compounds (HL1–HL4) were observed as a broad band between 3000 and 3200 cm^{-1}. In FTIR spectra of the oxime compounds (HL1ox–HL4ox), the carbonyl group stretching ($\acute{\imath}_{C=O}$) completely disappeared and a new sharp peak due to the imine bond ($\acute{\imath}_{C=N}$) was observed in the 1610–1638 cm^{-1} range. The rest of the stretching peaks of HL1ox–HL4ox are similar to those of the HL1–HL4 compounds.

2.3. X-ray structure of the HL1ox–HL3ox compounds

Single crystals of HL1ox were obtained from slow evaporation of an acetone solution of the compound. The molecular structure of the compound in the solid state was determined by XRD study. The molecular structure of the compound is solved in the monoclinic crystal system and $P2_1/c$ space group. The molecular structure of the compound is given in Figure 3.

The bond lengths of diazo (N2=N3) and azomethine (C1=N1) groups in the compounds are 1.275(12) and 1.234(11) Å, respectively. The phenyl and phenol rings in the molecule are translocated with respect to the diazo group. There is a phenol-imine intramolecular (O1H$\cdots$N1) hydrogen bond in the molecule. In addition to the intramolecular phenol-imine hydrogen bond, the phenol-imine molecule forms a dimer with two complementary hydrogen bonds of two azo-oxime molecules, as shown in Figure 4.[13,14] In the structure, dimeric molecules are further linked by $\pi - \pi$ interactions.

The HL2ox compound was recrystallized from EtOH solution. The structure of the compound was solved in the monoclinic crystal system and $P2_1/n$ space group. The X-ray structure of HL2ox is given in Figure 3. The

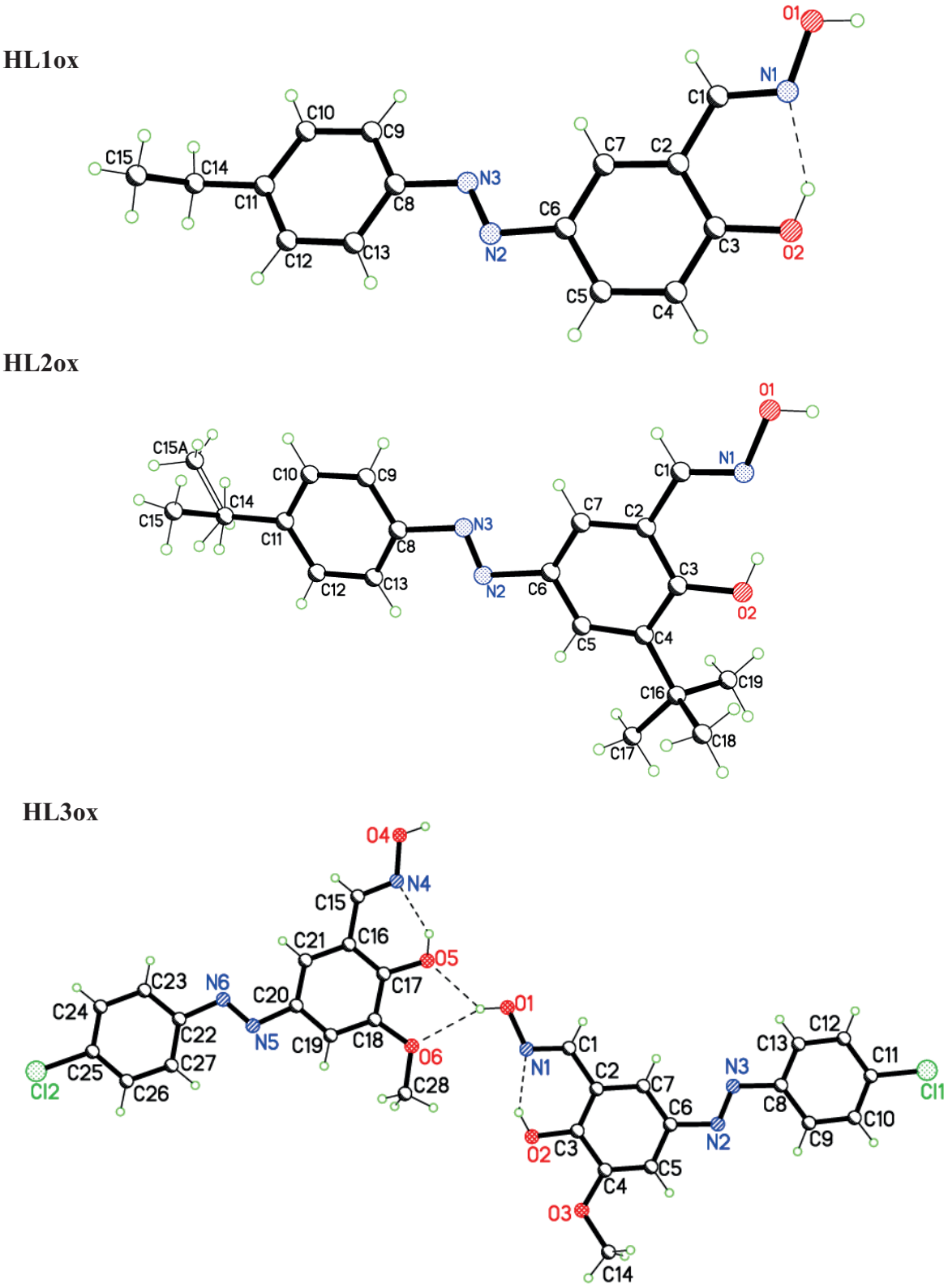

Figure 3. X-ray structures of HL1ox–HL3ox compounds with atom numbering. Hydrogen bonds in HL3ox are shown as dashed lines.

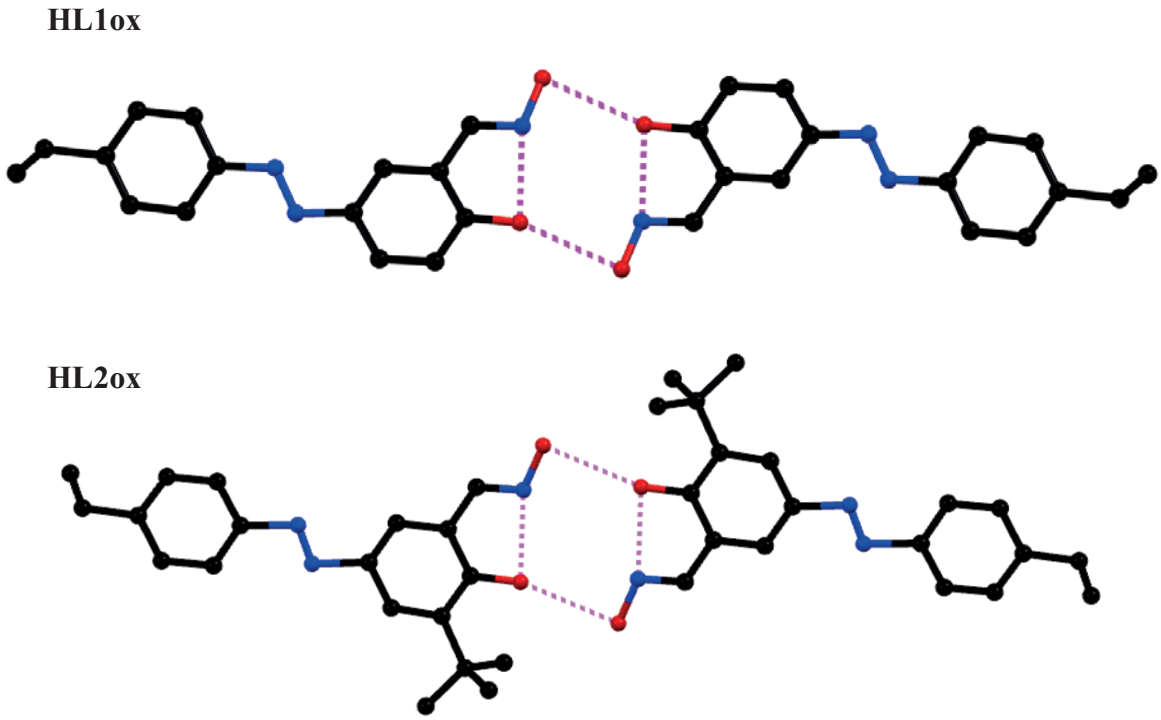

Figure 4. Hydrogen bonded dimers in HL1ox and HL2ox.

bond lengths of diazo (N2=N3) and azomethine (C=N) groups are 1.144(7) and 1.277(8) Å, respectively. As expected, there is a phenol-imine intramolecular (O1H$\cdots$N1) hydrogen bond. In the structure of the compound, the ethyl group of the C8/C13 phenyl ring is disordered and this was modeled over two positions. The oxime oxygen group (as hydrogen bond donor) makes a hydrogen bond with a phenolic oxygen atom of a neighboring molecule (hydrogen bond acceptor), resulting in a hydrogen bonded dimer (Figure 4). The $\pi-\pi$ interactions between the phenol rings (centroid-centroid distance between phenol rings is 3.808 Å) of the dimeric molecules were observed.

Single crystals of HL3ox suitable for single-crystal XRD study were obtained from slow evaporation of MeOH solution of the compound. The X-ray structure of the compound is given in Figure 3. In the structure of the compound, there were two molecules in the asymmetric unit. These two molecules in the asymmetric unit exhibit small differences between the dihedral of the phenyl rings in the molecules with similar bond angles and distances. The azomethine (C=N) and diazo (N=N) bond lengths in both molecules in the asymmetric unit are within the expected limits. In the structure of the molecule, there is a phenol-imine hydrogen bond (OH$\cdots$N). In the structure, hydrogen bond chains are formed by hydrogen bonds between the oxime group (hydrogen bond donor) and the phenolic and methoxy group oxygen atoms (hydrogen bond acceptor). The structure of the compound is further stabilized by the $\pi-\pi$ phenyl-phenyl interactions (centroid-centroid distance between phenol and phenyl rings is 3.919 Å).

Hirshfeld surface analysis is a common tool to investigate the nature of intermolecular interactions within crystal packing. The Hirshfeld surfaces for HL1ox–HL3ox were obtained for visualizing the van der Waals distances and determining the interaction sites within the structures.[15] The surfaces for the oxime compounds

were obtained using Crystal Explorer software, which uses X-ray crystallographic data in CIF format.[16] The fingerprint plots of the compounds show two large spikes for the (H$\cdots$O/O$\cdots$H) contacts to the adjacent molecules. The fingerprint plot of HL1ox is shown in Figure 5. The hydrogen bond contacts in the compounds are seen as intense red spots on the d_n surface. A cyclic hydrogen bond pattern is usually shown by a large number of fused spots between the main spikes.

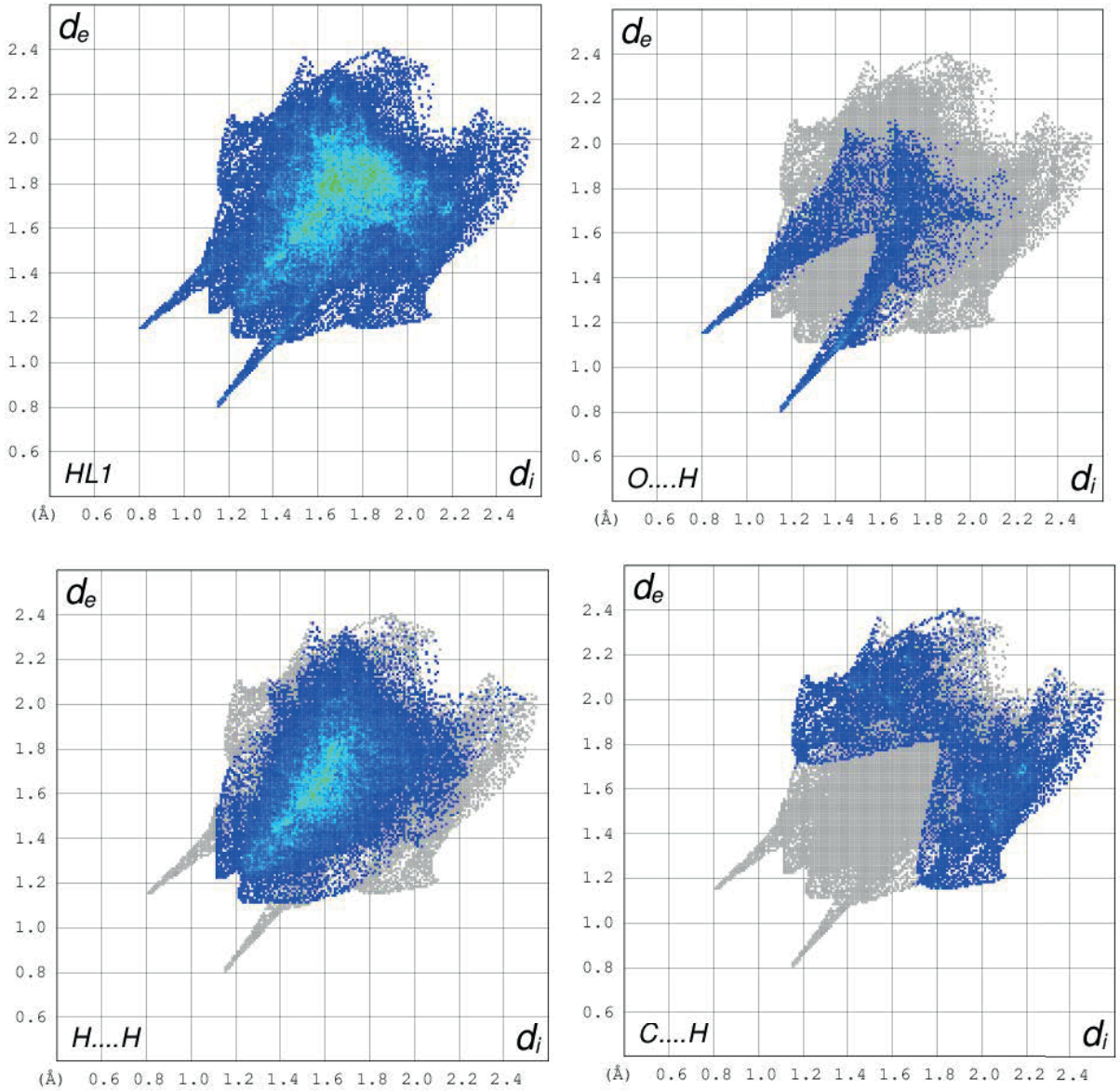

Figure 5. Fingerprint plots for HL1ox.

Relative contribution of the different contacts to the Hirshfeld surface of the HL1ox–HL3ox molecules were calculated. For the compounds, the largest contribution comes from H$\cdots$H contacts, followed by H$\cdots$O/O$\cdots$H and H$\cdots$C/C$\cdots$H contacts. The H$\cdots$N/N$\cdots$H contacts also play a role in the packing structure.

2.4. Computational studies

The mentioned ligands, HL1ox–HL4ox, in dimeric form and their metal complexes are optimized at B3LYP/6–31G(LANL2DZ) level in gas phase. Optimized structures of dimeric ligands and $[Cu(L^1)_2]$, $[Cu(L^2)_2]$, $[Cu(L^3)_2]$, $[Cu(L^4)_2]$, $[Ni(L^3)_2]$, and $[Zn(L^3)_2]$ complex dimers were calculated. Dimeric ligand structures are investigated at B3LYP/6-31G level. There is a cavity in each dimer structure. Thermodynamic parameters of the mentioned complexes and the dimeric oxime ligands, which are total energy (E_{Total}), enthalpy energy (H), and Gibbs free energy (G), are given in Table 1.

Table 1. Thermodynamic parameters of related complexes' B3LYP/6-31G(LANL2DZ) levels in gas phase.

Complexes	E^a_{Total}	H^a	G^a	ΔE^b	ΔH^b
$[Cu(L^1)_2]$	–1984.474234	–1984.47329	–1984.58756	–2778.22	–2783.17
$[Cu(L^2)_2]$	–2298.659375	–2298.658431	–2298.793701	–2746.81	–2751.77
$[Cu(L^3)_2]$	–2975.426906	–2975.425962	–2975.544023	–2747.21	–2752.17
$[Ni(L^3)_2]$	–2948.615301	–2948.614356	–2948.729978	–2989.34	–2994.3
$[Zn(L^3)_2]$	–2844.884784	–2844.88384	–2845.003789	–2475.27	–2480.23
$[Cu(L^4)_2]$	–2220.124186	–2220.123241	–2220.254032	–2775.72	–2780.68

According to Table 1, $[Cu(L^3)_2]$ is the most stable copper complex, while $[Cu(L^1)_2]$ is the best interacting complex. Additionally, $[Cu(L^1)_2]$ has the highest formation stability. As for the other complexes, represented as $M(L^4)_2$, the most stable complex is $[Cu(L^3)_2]$. Additionally, $[Ni(L^3)_2]$ is the best interacting complex and has the highest formation stability.

2.5. Investigation of absorption spectra of synthesized compounds

The absorption properties of the novel azo-aldehydes (HL1–HL4) and their oxime derivatives (HL1ox–HL4ox) were studied in DMF solution (10^{-5} M). UV-Vis spectra of the compounds are given in Figure 6.

Two broad absorption bands are observed in the UV-Vis spectra of the synthesized azo-aldehyde compounds (HL1–HL4). The broad and intense absorption bands observed in the range of 290–420 nm are assigned to the $\pi - \pi^*$ transitions of the π electrons present in the compounds. The second band in the 410–520 nm range can be due to the n-π^* transitions. The n-π^* electronic transitions in HL1–HL4 are absent in the UV-vis spectra of HL1ox–HL4ox. A single absorption band in the UV-Vis spectra of HL1ox–HL4ox was seen as a strong absorption band in the range of 306–420 nm. This absorption band is attributed to $\pi - \pi^*$ electronic transitions. In oxime compounds, the absorption bands due to the $\pi - \pi^*$ electronic transitions shifted to longer wavelengths (red shift) when compared to the same bands in the azo-aldehyde (HL1–HL4) compounds.

2.6. Solvent extraction studies of oxime compounds

The solvent extraction capacities of the new oxime compounds for Cu(II), Ni(II), and Zn(II) ions were investigated. The solvent extraction procedure is shown in Figure 7. Liquid-liquid extraction processes were investigated for Cu(II), Ni(II), and Zn(II) metal ions at a pH range of 0 to 5 (Figure 8). The synthesized oxime compounds were found to have extraction capacity even at very low pH. As the pH increases from 0 to 5, the extraction capacity of the oxime compounds increases. At pH 0, 30% of Cu(II) content was transferred from the

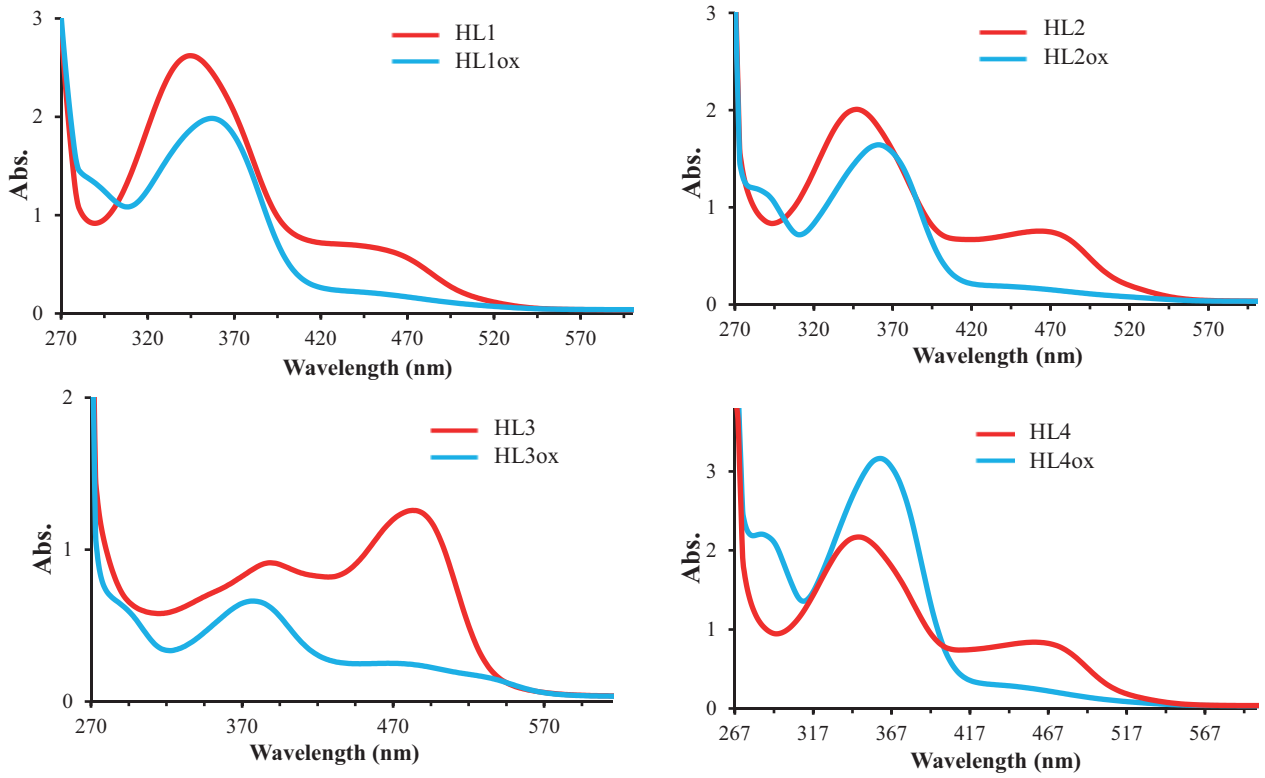

Figure 6. UV-Vis spectra of the compounds in DMF.

aqueous phase to the organic phase ($CHCl_3$). For the HL1ox compound, Ni(II) and Zn(II) ions showed very close extraction capacities between pH 0 and 5. For all oxime compounds at all pH values, Cu(II) ion shows higher extraction values than Ni(II) and Zn(II) ions. The vacancy formed by the dimerization of the oxime ligands is thought to be more suitable for Cu(II) ion, thus resulting in better extraction values (Figure 8).

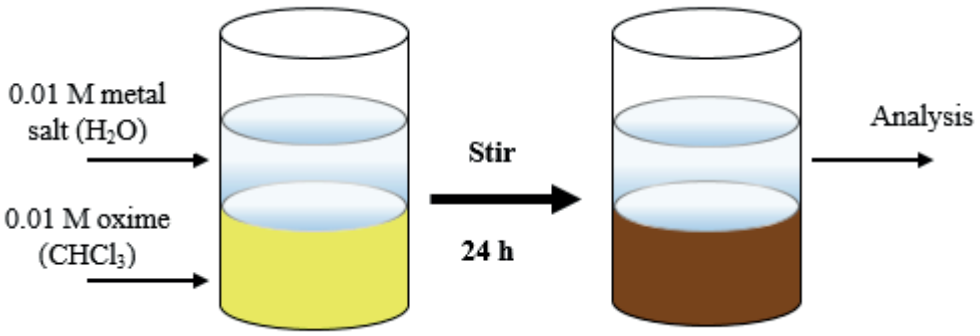

Figure 7. Schematic representation of liquid-liquid extraction.

Of the oxime ligands, the HL3ox compound was found to show the maximum extraction capacity for the Cu(II) ion at all pH values. In the HL1ox–HL4ox compounds, there are -H, -t-But, $-OCH_3$, and $-CH_3$ groups at the meta positions with respect to the oxime group (C=N-OH). In HL1ox, HL2ox, and HL4ox, the -C=N-OH group of oxime in the hydrogen bonded dimers does not interact with the groups at the meta positions, but the

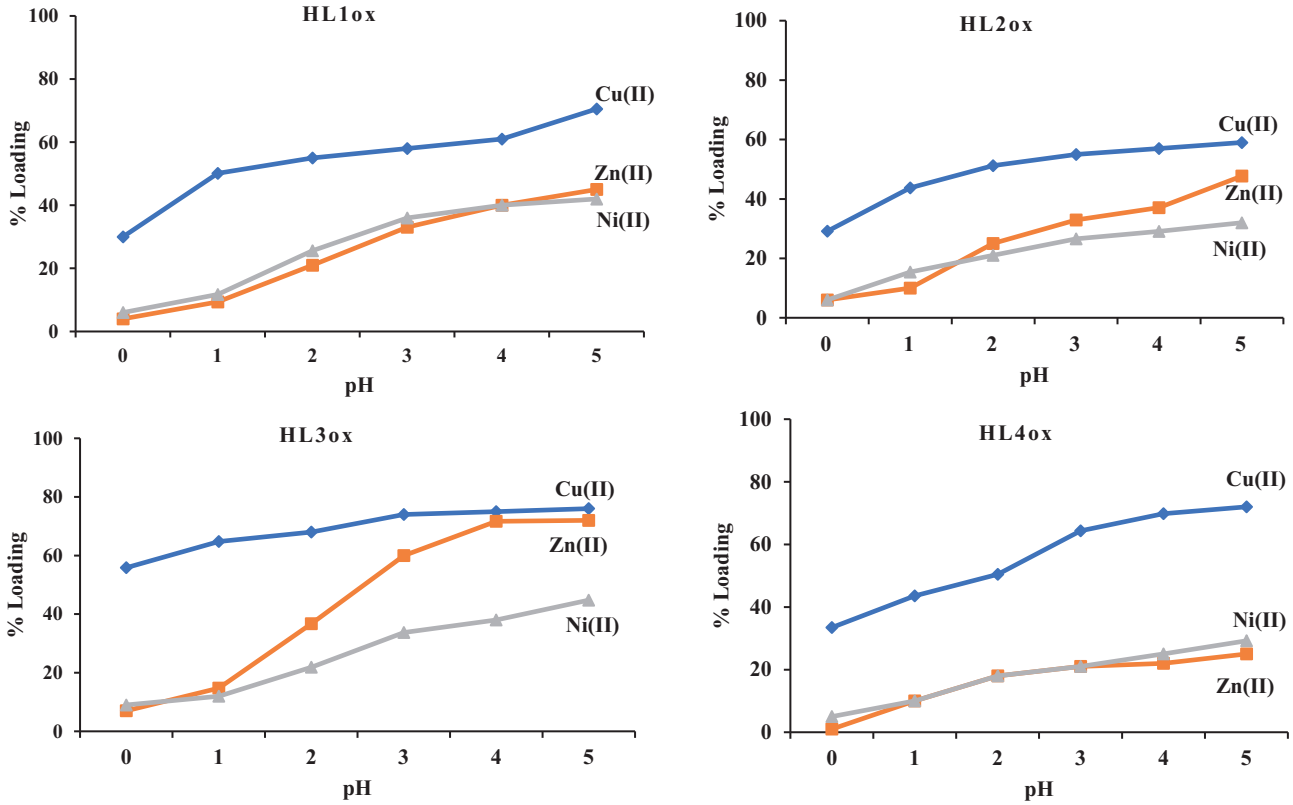

Figure 8. Cu/Ni/Zn(II) loading of chloroform solutions of HL1ox–HL4ox as a function of the equilibrium pH of the aqueous phase.

methoxy group of HL3ox enters into weak hydrogen bond interaction with the oxime group of the neighboring molecule.[17,18] These weak hydrogen bond interactions are thought to contribute to the overall stability of the resulting complex.[17,18] When the extraction results are examined, it is found that HL1ox, HL2ox, and HL4ox have about 30% extraction capacities at pH 0, while HL3ox has about 55% extraction capacity. In the Cu(II) extraction for the HL3ox compound, 75% extraction was obtained at pH 3 and this did not show considerable change at pH 4 and pH 5 (Figure 8). When the results of extraction studies are examined, 100% extraction was not observed for Cu(II), Zn(II), or Ni(II) ions. The transfer of metal ions to the organic phase was due to the coordination of the ligands to the metal ions. During the complexation, there are two possible 1:2 and 1:1 (metal:ligand) complexations. If only the 1:1 (metal:ligand) complex forms, then all of the metal ions will have been extracted. If only the 1:2 (metal:ligand) complexations have formed, then 50% of the metal ions will have been retained in aqueous solutions. In the solvent extraction study of Cu(II), more than 50% of Cu(II) (pH 1–5) was transferred to the organic phase. This suggests that both 1:1 and 1:2 complexations formed in the recovery process.

In order to compare the stability of the complexes with the extraction capacities, the thermodynamic parameters [energy (E_{Total}), enthalpy energy (H), and Gibbs free energy (G)] for the possible structures [$M(L_{oxime})_2$] (M = Cu, Ni, or Zn) were calculated. According to the thermodynamic parameters, [$Cu(L^3)_2$] is the most stable complex among the studied compounds. The lower Gibbs free energy (G) of complex [$Cu(L^3)_2$] resulted in better extraction capacity for the complex.

Time-dependent extraction study of Cu(II) was done for the HL3ox ligand at pH 5. In the end of the first 15 min, almost 30% of Cu(II) was removed from the aqueous solution and the extraction reached a maximum at 60 min with over 70% extraction. After 60 min, the extraction capacity of HL3ox did not show considerable change. To compare the selectivity of HL3ox, competing experiments were also carried out at pH 5 for 120 min. The Cu(II)/Ni(II), Cu(II)/Zn(II), and Cu(II)/Ni(II)/Zn(II) stock solutions were extracted with chloroform solutions containing HL3ox (0.01 M). The extraction values are expressed as % extraction and shown in Figure 9. For all three competing experiments, Cu(II) showed better extraction values, confirming the selectivity of HL3ox for Cu(II).

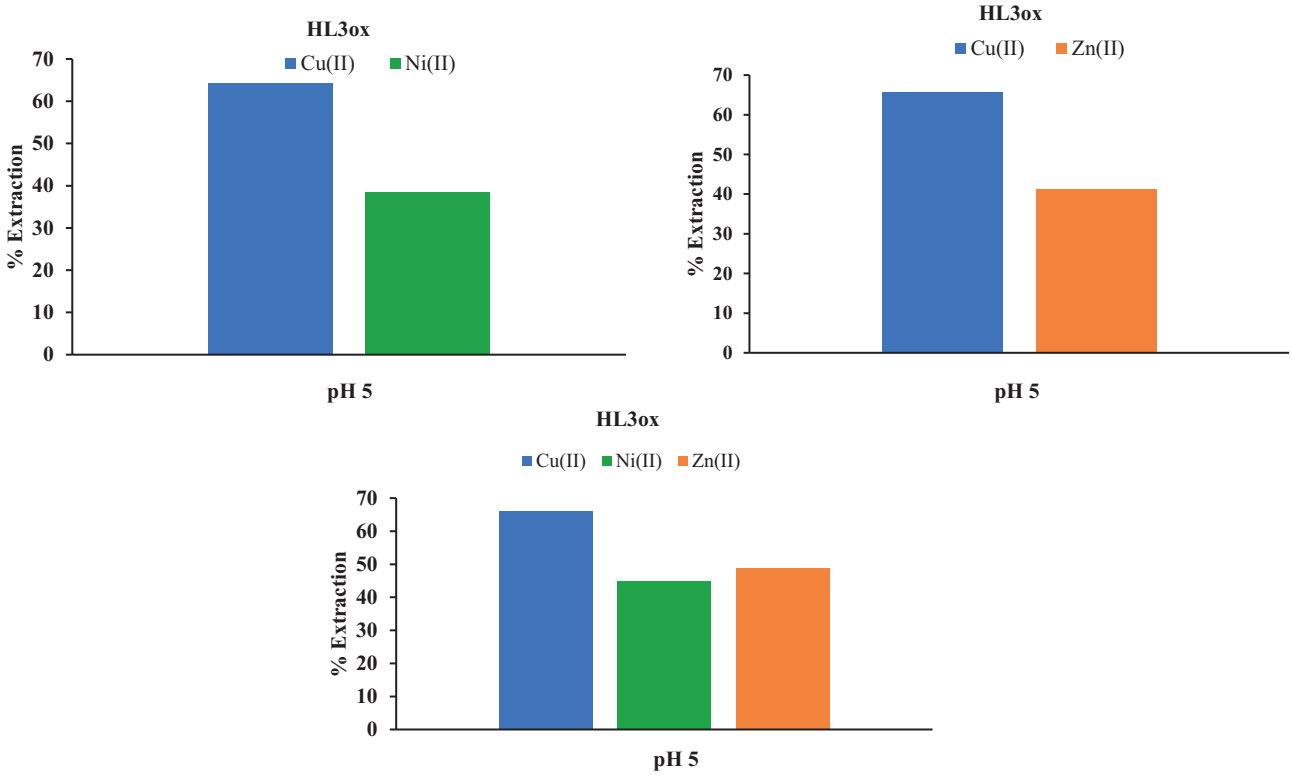

Figure 9. Liquid-liquid extraction for Cu(II)/Ni(II), Cu(II)/Zn(II), and Cu(II)/Ni(II)/Zn(II) mixed solutions.

2.7. Conclusions

In this work, four new azo-aldehyde compounds (HL1–HL4) were synthesized by diazo coupling reactions. Subsequently, *p*-substituted phenolic oxime compounds (HL1ox–HL4ox) were synthesized by reacting the synthesized azo-aldehyde compounds with hydroxylamine. Solid-state structures of HL1ox–HL3ox were determined by single-crystal XRD studies. Absorption properties of the synthesized azo-aldehyde and oxime compounds were investigated in DMF. Finally, the HL1ox–HL4ox compounds were used for solvent extraction of metal ions. The HL1ox–HL4ox ligands showed higher extraction performance for Cu(II) ion than Ni(II) and Zn(II) ions. The effect of pH on extraction was investigated and it was found that the synthesized oxime compounds could extract at even as low as pH as 1. When the results were examined, the -OMe group in the meta position of the HL3ox compound increased its extraction capacity. For industrial applications, the HL3ox compound can be used for the liquid-liquid extraction of Cu(II) from aqueous solutions. Computational studies of the

mentioned compounds were performed by B3LYP method. Thermodynamic parameters of related complexes were examined in detail. Formation enthalpy and interaction energy for each complex were calculated and examined.

3. Experimental

3.1. Materials

4-Ethylaniline, 4-chloroaniline, 2-hydroxybenzaldehyde, 3-tert-butyl-2-hydroxybenzaldehyde, sodium nitrite, $CuSO_4.5H_2O$, $NiSO_4.6H_2O$, and $ZnSO_4.7H_2O$ were purchased from Aldrich Chemical Company and used as received. 4-tert-Butylaniline, 2-hydroxy-3-methoxybenzaldehyde, 2-hydroxy-3-methylbenzaldehyde, and hydroxylamine hydrochloride were purchased from Acros Organics Chemical Company and used as received. All other materials used were of reagent grade quality, provided from chemical companies and used as received without further purification.

3.2. Physical measurements

NMR spectra were obtained using a Bruker Advance III 400 MHz spectrometer. The FTIR spectra were obtained (4000–450 cm^{-1}) using a PerkinElmer spectrum 400 FTIR spectrophotometer. The absorption spectra in the 200–800 nm range were obtained on a Shimadzu UV-160A UV-Vis spectrophotometer. Solid-state structures of HL1ox, HL2ox, and HL3ox were determined using a Bruker D8 QUEST diffractometer. Efficacy of the new *p*-substituted phenolic oxime ligands for recovery of metal ions was determined by PerkinElmer Optima 2100 DV ICP-OES.

3.3. Synthesis of azo-aldehyde ligands HL1–HL4

Azo-aldehyde compounds HL1–HL4 were synthesized according to the reported method.[19,20] 4-Substituted aniline derivatives (10 mmol) were mixed with 50 mL of water. To this solution, concentrated HCl (2.5 mL) was added and the solution was filtered. The solution was then cooled on an ice bath (0–5 °C), followed by slow addition of $NaNO_2$ (13.9 mmol) in water (2 mL). The reaction solution was kept for 30 min in an ice bath. To the ice-cold solution, corresponding salicylaldehyde derivatives (10 mmol) in 10% NaOH solution (10 mL) were added dropwise and the reaction mixture was stirred for 2 h at room temperature. Upon addition of salicylaldehyde derivatives, the formed yellow precipitate was filtered under vacuum, washed with water (15 mL), and dried in air.

HL1: Yellow powder, yield: 1.261 g, 5 mmol (49.6%). Mp 116–120 °C. NMR ($CDCl_3$, ä ppm): ^{1}H, 11.33 (s, 1H, OH), 10.02 (s, 1H, CH=O), 8.18 (s, 1H, aromatic CH), 8.17 (d, H, aromatic CH), 7.85 (d, 2H, aromatic CH), 7.37 (d, 2H, aromatic CH), 7.13 (d, H, aromatic CH), 2.76 (q, 2H, ethyl group protons -CH_2-), 1.32 (t, 3H, ethyl group protons –CH_3). ^{13}C, 196.60 (C=O), 163.52, 150.59, 147.94, 145.99, 130.67, 129.08, 128.64, 122.8, 120.3, 118.5 (aromatic C atoms), 28.86 and 15.40 (ethyl group C atoms). IR (ATR, cm^{-1}): $3194_{((O-H))}$, $2959_{((C-H))}$, $1652_{((C=O))}$, $1455_{((N=N))}$.

HL2: Brown powder, yield: 1.0285 g, 3.3 mmol (66.4 %). Mp 92–96 °C. NMR ($CDCl_3$, äppm): ^{1}H, 12.15 (s, 1H, OH), 10.01 (s, 1H, CH=O), 8.23 (s, 1H, aromatic CH), 8.04 (s, 1H, aromatic CH), 7.87 (d, 2H, aromatic CH), 7.37 (d, 2H, aromatic CH), 1.53 (s, 9H, *tert*-butyl group protons –$C(CH_3)_3$), 2.77 (q, 2H, ethyl group protons -CH_2-), 1.33 (t, 3H, ethyl group protons –CH_3). ^{13}C, 197.28 (C=O), 163.28, 150.77, 147.66,

145.31, 139.45, 128.61, 126.72, 122.80, 120.34 (aromatic C atoms), 35.20 and 29.18 (*tert*-butyl group C atoms), 28.86 and 15.42 (ethyl group C atoms). IR (ATR, cm^{-1}): $2955_{((C-H))}$, $1646_{((C=O)}$, $1426_{((N=N))}$.

HL3: Brown powder, yield: 1.1000 g, 3.78 mmol (75.8 %). Mp 178–182 °C. NMR ($CDCl_3$, ä ppm): ^{1}H, 10.05 (s, 1H, CH=O), 7.87 (d, 2H, aromatic CH), 7.73 (s, 1H, aromatic CH), 7.50 (d, 2H, aromatic CH), 7.29 (s, H, aromatic CH), 4.03 (s, 3H, methoxy group protons –OCH_3). ^{13}C, 196.35 (C=O), 154.69, 150.65, 149.31, 145.39, 136.92, 129.43, 124.55, 124.02, 123.94, 119.95, 119.58, 117.92 (aromatic C atoms), 56.40 (methoxy C atom). IR (ATR, cm^{-1}): $3088_{((O-H))}$, $1666_{((C=O))}$, $1426_{((N=N))}$.

HL4: Yellow powder, yield: 2.2578 g, 7.6 mmol (76.2 %). Mp 102–106 °C. NMR ($CDCl_3$, ä ppm): ^{1}H, 11.62 (s, 1H, OH), 10.01 (s, 1H, CH=O), 8.05 (s, 1H, aromatic CH), 7.86 (d, 2H, aromatic CH), 7.57 (d, 2H, aromatic CH), 2.38 (s, 3H, methyl group protons -CH_3), 1.41 (s, 9H, *tert*-butyl group protons –$C(CH_3)_3$). ^{13}C, 196.73 (C=O), 162.16, 154.53, 150.37, 145.49, 130.50, 128.09, 127.59, 126.09, 122.45, 119.66 (aromatic C atoms), 35.04 and 31.29 (*tert*-butyl group C atoms), 15.25 (methyl group C atoms). IR (ATR, cm^{-1}): $2957_{((C-H))}$, $1651_{((C=O))}$, $1442_{((N=N))}$.

3.4. Synthesis of azo-oxime compounds HL1ox–HL4ox

The azo-aldehyde compounds (1.000 g, 3.9 mmol for HL1; 1.000 g, 3.2 mmol for HL2; 1.000 g, 3.4 mmol for HL3 and HL4) were dissolved in EtOH (100 mL). Then NaOAc (0.8 g for HL1, 0.66 for HL2, 0.70 g for HL3 and HL4, excess amounts) and NH_2OH.HCI (0.68 g for HL1, 0.56 for HL2, 0.59 g for HL3 and HL4, excess amounts) were added to the solutions[21,22] and refluxed for 2 h. The reaction mixture was then poured into ice-cooled water (250 mL) and precipitates were collected by filtration and dried in air.

HL1ox: Yellow crystals, yield: 0.5163 g, 1.92 mmol (49.16%). Mp 130–140 °C. NMR ($CDCl_3$, ä ppm): ^{1}H, 10.28 (s, 1H, OH), 8.36 (s, 1H, CH=N-O), 7.96 (d, H, aromatic CH), 7.94 (s, 1H, aromatic CH), 7.84 (d, 2H, aromatic CH), 7.36 (d, 2H, aromatic CH), 7.13 (d, 1H), 2.76 (q, 2H, ethyl group protons -CH_2-), 1.31 (t, 3H, ethyl group protons –CH_3). ^{13}C, 159.65 (C=N-OH), 152.70, 150.78, 147.56, 146.12, 128.61, 125.97, 125.81, 122.72, 117.51, 116.59 (aromatic C atoms), 28.84 and 15.41 (ethyl group carbon atoms). IR (ATR, cm^{-1}): $3411_{((O-H))}$, $2965_{((C-H))}$, $1612_{((C=N))}$, $1448_{((N=N)}$.

HL2ox: Orange crystals, yield: 0.3815 g, 1.17 mmol (36.64%). Mp 155–165 °C. NMR ($CDCl_3$, ä ppm): ^{1}H, 10.79 (s, 1H, OH), 8.37 (s, 1H, CH=N-O), 8.0 (s, 1H, aromatic CH), 7.84 (d, 2H, aromatic CH), 7.71 (s, 1H, aromatic CH), 7.37 (d, 2H, aromatic CH), 1.52 (s, 9H, *tert*-butyl group protons –$C(CH_3)_3$), 2.75 (q, 2H, ethyl group protons -CH_2-), 1.31 (t, 3H, ethyl group protons –CH_3). ^{13}C, 159.16 (C=N-OH), 153.42, 150.94, 147.22, 145.40, 138.22, 128.56, 124.16, 123.57, 122.61, 116.84 (aromatic C atoms), 35.21 and 29.31 (*tert*-butyl group carbon atoms), 28.81 and 15.42 (ethyl group carbon atoms). IR (ATR, cm^{-1}): $3438_{((O-H))}$, $2968_{((C-H))}$, $1638_{((C=N))}$, $1454_{(((N=N))}$.

HL3ox: Brown crystals, yield: 0.2904 g, 0.95 mmol (27.86%). Mp 213–223 °C. NMR ($CDCl_3$, ä ppm): ^{1}H, 10.35 (s, 1H, OH), 8.38 (s, 1H, CH=N-O), 7.87 (s, 1H, aromatic CH), 7.58 (d, 2H, aromatic CH), 7.51 (s, 1H, aromatic CH), 7.28 (d, 2H, aromatic CH), 4.03 (s, 3H, methoxy group protons –OCH_3). IR (ATR, cm^{-1}): $3416_{((O-H))}$, $1610_{((C=N))}$, $1434_{((N=N))}$.

HL4ox: Yellow powder, yield: 0.4462 g, 1.43 mmol (42.15 %). Mp 133–143 °C. NMR ($CDCl_3$, ä ppm): ^{1}H, 10.52 (s, 1H, OH), 8.36 (s, 1H, CH=N-O), 7.85 (d, 2H, aromatic CH), 7.72 (s, H, aromatic CH), 7.56 (d,

2H, aromatic CH), 2.39 (s, 3H, methyl group protons -CH_3), 1.41 (s, 9H, *tert*-butyl group protons –$C(CH_3)_3$). ^{13}C, 158.09 (C=N-OH), 154.19, 152.86, 150.51, 145.68, 126.88, 126.08, 125.97, 124.62, 122.31, 115.90 (aromatic C atoms), 35.01 and 31.30 (*tert*-butyl group C atoms), 15.96 (methyl group C atoms). IR (ATR, cm^{-1}): $3400_{((O-H))}$, $2953_{((C-H))}$, $1632_{((C=N))}$, $1427_{((N=N))}$.

3.5. X-ray structure solution and refinement

X-ray crystallographic data for oxime compounds HL1ox, HL2ox, and HL3ox were collected at 293(2) K on a Bruker D8 QUEST diffractometer using Mo-$K\alpha$ radiation (1 = 0.71073 Å). Data reduction was performed using Bruker SAINT.[23,24] SHELXS97 was used to solve and SHELXL2014/6 to refine the structures.[25,26] The structures were solved by direct methods and refined on F^2 using all the reflections. All the nonhydrogen atoms were refined using anisotropic atomic displacement parameters and hydrogen atoms bonded to carbon and oxygen atoms were fixed at calculated positions using a riding model and refined with temperature factors. The crystal data and refinement details for HL1ox, HL2ox, and HL3ox are given in Table 2.

3.6. Solvent extraction experiments of HL1ox–HL4ox compounds

Stock solutions (0.01 M) of the oxime ligands (HL1ox, HL2ox, HL3ox, and HL4ox) were prepared in chloroform. Aqueous stock solutions (0.01 M) of Cu(II), Ni(II), and Zn(II) were prepared from their sulfate salts. To adjust the pH of metal solutions, 0.1 M NaOH and 0.5 M H_2SO_4 solutions were prepared. All extractions were performed according to the same general procedure. Solutions of ligands (0.01 M) in chloroform (5 mL) were added to 0.01 M metal aqueous solutions (5 mL), which were adjusted to different pH values and stirred for 24 h at room temperature.[11] After the phase separations, aliquots of 0.1 mL of the aqueous phase were separated for metal analysis by ICP-OES. From the results obtained, the content of metal transferred from the aqueous phase to the organic phase ($CHCl_3$) was calculated as % and graphically plotted against pH.

3.7. Computational method

GaussView 5.0.9 and Gaussian 09 AS64L-G09RevD.01 package programs were used to carry out quantum chemical calculations.[27,28] B3LYP, which is one of the hybrid density functional theory functions, was selected as the method for the investigated molecules. As basis sets, LANL2DZ was selected for metal atoms and 6–31G was selected for the rest of the atoms in the complexes. No imaginary frequency was obtained from calculations. Additionally, organic compounds were calculated at B3LYP/6-31G level in vacuum. Optimized structures of related compounds were taken via the Chemcraft Version 1.8 software program.[29] Interaction energies and formation enthalpy of the complexes are calculated by using Eqs. (1) and (2), respectively.

$$\Delta E = E_{Complex} - E_{Metal} - E_{Ligands} \tag{1}$$

$$\Delta H = H_{Complex} - H_{Metal} - H_{Ligands} \tag{2}$$

Table 2. X-ray crystallographic data for the compounds.

Compound	HL1ox	HL2ox	HL3ox
Formulae	$C_{15}H_{15}N_3O_2$	$C_{19}H_{23}N_3O_2$	$C_{14}H_{12}ClN_3O_3$
Molecular weight	269.30	325.40	305.72
Temperature	293(2) K	293(2) K	293(2) K
Wavelength	0.71073 Å	0.71073 Å	0.71073 Å
Unit cell	*Monoclinic*	*Monoclinic*	*Orthorhombic*
Space group	$P2_1/c$	$P2_1/n$	$Pca2_1$
	a = 21.307(4) Åα = 90°	a = 12.107(2) Åα = 90°	a = 7.3775(12) Å α = 90°
	b = 5.0017(9) Åβ = 100.454(10)°	b = 9.0979(15) Åβ = 90.630(6)°	b = 17.996(4) Å β = 90°
	c = 13.203(3) Åγ = 90°	c = 16.366(3)Åγ = 90°	c = 20.817(4) Å γ = 90°
Volume (Å^3)	1383.7(4)	1802.6(5)	2763.8(9)
Z	4	4	8
Density(calc.) (Mg/m^3)	1.293	1.119	1.469
Absorption coefficient (mm^{-1})	0.088	0.079	0.290
Crystal size (mm^3)	0.15 × 0.11 × 0.09	0.13 × 0.12 × 0.11	0.14 × 0.10 × 0.09
Ref. collected	2975	22489	28728
Indepent ref.	1669 [R(int) = 0.0538]	3387 [R(int) = 0.0806]	5265 [R(int) = 0.0904]
Final R values [I>2sigma(I)]	R1 = 0.1366, wR2 = 02530	R1 = 0.143, wR2 = 02534	R1 = 0.0837, wR2 = 0.1566
R indixes (all data)	R1 = 0.2389, wR2 = 0.3083	R1 = 0.2096, wR2 = 0.2798	R1 = 0.1209, wR2 = 0.1703
CCDC Number	1835647	1835648	1835649

Acknowledgments

The authors are grateful to the Kahramanmaraş Sütçü İmam University Science Projects Unit for the financial support for this study (Project Number: 2017/1-49 YLS). The authors also acknowledge the Scientific and Technological Research Application and Research Center, Sinop University, Turkey, for use of the Bruker D8 QUEST diffractometer.

References

1. Wilson, A. M.; Bailey, P. J.; Tasker, P. A.; Turkington, J. R.; Grant, R. A.; Love, J. B. *Chem. Soc. Rev.* **2014**, *43*, 123-134.
2. Habashi, F. *Hydrometallurgy* **2005**, *79*, 15-22.
3. Flett, D. S. *J. Chem. Technol. Biotechnol.* **1999**, *74*, 99-105.
4. Mézard, M.; Parisi, G.; Virasoro, M. *Spin Glass Theory and Beyond*; World Scientific Publishing Company: Singapore, 1987.
5. Tasker, P. A.; Tong, C. C.; Westra, A. N. *Coord. Chem. Rev.* **2007**, *251*, 1868-1877.
6. Turkington, J. R.; Bailey, P. J.; Love, J. B.; Wilson, A. M.; Tasker, P. A. *Chem. Comm.* **2013**, *49*, 1891-1899.
7. Kordosky, G. A. *J. South African Inst. Min.* **2002**, *102*, 445-450.
8. Moore, R. H.; Partridge, J. A. *Batelle Pacific Northwest Laboratories Report (No. BNWL-SA-4476; CONF-721214-1)*; Pacific Northwest Laboratories: Batelle, WA, USA, 1972.
9. Zhu, S.; Hu, H.; Hu, J.; Li, J.; Hu, F.; Wang, Y. J. *Mol. Struc.* **2017**, *1144*, 191-198.
10. Smith, A. G.; Tasker, P. A.; White, D. J. *Coord. Chem. Rev.* **2003**, *241*, 61-85.
11. Forgan, R. S.; Wood, P. A.; Campbell, J.; Henderson, D. K.; McAllister, F. E.; Parsons, S.; Pidcock, E.; Swart, R. B.; Tasker, P. A. *Chem. Commun.* **2007**, *46*, 4940-4942.
12. Hoang, A. S.; Tran, T. H.; Nguyen, H. N.; Vu, H. S.; Vo, T. P.; Phan, C.; Nguyen, T. V. *Korean J. Chem. Eng.* **2015**, *32*, 1598-1605.
13. Manimekalai, A.; Balachander, R. *J. Mol. Struc.* **2012**, *1027*, 175-185.
14. Premuzic, D.; Filarowski, A.; Hołyńska, *M. J. Mol. Struc.* **2017**, *1136*, 100-106.
15. Spackman, M. A.; Jayatilaka, D. *Cryst. Eng. Comm.* **2009**, *11*, 19-32.
16. Bernstein, J.; Davis, R. E.; Shimoni, L.; Chang, N. L. *Angew. Chemie Int. Ed. Eng.* **1995**, *34*, 1555-1573.
17. Forgan, R. S. *Inorg. Chem.* **2011**, *50*, 4515-4522.
18. Roach, B. D. *Aust. J. Chem.* **2017**, *70*, 556-565.
19. Eren, T.; Kose, M.; Sayin, K.; McKee, V.; Kurtoglu, M. *J. Mol. Struct.* **2014**, *1065*, 191-198.
20. Cabir, B.; Avar, B.; Gülcan, M.; Kayraldız, A.; Kurtoğlu, M. *Turk. J. Chem.* **2013**, *37*, 422-438.
21. Köse, M.; Kurtoglu, N.; Gümüşsu, Ö.; Tutak, M.; McKee, V.; Karakaş, D.; Kurtoglu, M. *J. Mol. Struct.* **2013**, *1053*, 89-99.
22. Bitmez, Ş.; Sayin, K., Avar, B.; Köse, M.; Kayraldız, A.; Kurtoğlu, M. *J. Mol. Struct.* **2014**, *1076*, 213-226.
23. Bruker Inc. *APEX2 and SAINT*. Bruker AXS Inc.: Madison, WI, USA, 1998.
24. Bruker Inc. *A. P. E. X. Saint and SADABS*. Bruker Inc.: Madison, WI, USA, 2009.
25. Sheldrick, G. M. *Acta Crystallogr. Sect. A Found. Crystallogr.* **2008**, *64*, 112-122.
26. Sheldrick, G. M. *Acta Crystallogr. Sect. C Struct. Chem.* **2015**, *71*, 3-8.
27. Dennington, R.; Keith, T.; Millam, J. *Gauss View*; Semichem Inc.: Shawnee Mission, KS, USA, 2009.
28. Frisch, M. J. *Gaussian 09 Revision D. 01*; Gaussian Inc.: Wallingford, CT, USA, 2009.
29. Zhurko, G. A.; Zhurko, D. A. *ChemCraft 1.8*, 2009.